JOURNAL OF MATERIALS SCIENCE 23 (1988) 1260–1264

Effect of crystalline properties on coercive force in iron acicular fine particles

FUMIO WATARI*, KOICHI HANEDA, KEIJI YADA
Research Institute for Scientific Measurements, Tohoku University, 2-1-1 Katahira, Sendai 980, Japan

Crystallographic properties and their size dependence in acicular fine particles of iron prepared by reduction from α-FeOOH were investigated by transmission electron microscopy and compared with magnetic properties. Although both larger particles with an average needle length of 0.5 μm and smaller ones of 0.2 μm length have single domain configuration, the former are crystallographically polycrystalline while the latter are single crystal with a [1 0 0] axial orientation, an easy magnetization direction of iron. The coercive force, principally yielded by external shape anisotropy, is higher in smaller particles in spite of their inferior axial ratio. The intrinsic magnetocrystalline anisotropy is inferred to be the most responsible to give rise to this further increase of coercive force. The experimentally obtained values of magnetic properties are also compared with the theoretical estimation, which results semi-quantitatively in good accordance.

1. Introduction

Magnetic tapes use, as recording media, acicular fine particles which make use of shape anisotropy to yield coercive force [1]. In order to make needle shapes, α-FeOOH (goethite) [2] is used as a starting material. Through the processes of dehydration [3–7], reduction and oxidation, it is reduced to γ-Fe_2O_3 (maghaemite) [8] and increasingly down to iron (metal iron) in recent years. In the case of γ-Fe_2O_3 there is an orientation relation between starting material and product [9, 10]. For the case of iron, it is unknown whether there is definite orientation relation like γ-Fe_2O_3.

The present study aims to examine the orientation relation of iron acicular fine particles and its size dependence and to investigate the relation between crystallographic properties and magnetic properties.

2. Experimental procedure

The different sizes of starting material, goethite α-FeOOH (1 and 0.5 μm average needle length), were prepared and reduced under isothermal heat treatment at 400° C in a hydrogen atmosphere. Treatment for 2 h could give rise to the complete conversion to the metal iron product. The estimation of particle size was done by electron microscopy, and the average size of the iron particles produced was 24 × 24 × 500 nm^3 (specimen A) and 20 × 20 × 200 nm^3 (specimen B).

Observation was done by a 200 kV transmission electron microscope with a side entry rotation-tilt holder. The tilting axis was aligned parallel and perpendicular to the needle axis of a single particle. The electron micrographs and selected-area electron diffraction patterns were then taken at various tilting angles. From these diffraction patterns, the three-dimensional reciprocal lattice was constructed and then identification of products and determination of the orientation relation were carried out.

The magnetization curve was measured by the vibrating sample magnetometer method. The magnetic field was applied at maximum 10 kOe, which yielded a magnetic moment several per cent smaller than the saturation magnetization realized approximately at 15 kOe.

3. Experimental results

The change in magnetic properties by isothermal reduction in a hydrogen atmosphere is shown in Fig. 1. The products are of the series starting from α-FeOOH (1 μm size) leading to iron (specimen A: 0.5 μm) after 2 h treatment. Saturation magnetization, σ_s, squareness ratio, σ_r/σ_s (σ_r = remanent magnetization) and coercive force, H_c, are all increased with the 400° C heat-treatment time. From observation by electron microscopy, it is confirmed that 2 h reduction treatment is enough to convert fine particles completely to metal iron. At shorter reduction time, electron diffraction shows the existence of oxides whose structure and occupancy ratio depend on treatment time. By reduction down to metal iron, coercive force in particular is improved considerably compared with the state of iron oxide. For the 2 h heat treatment the values of both A and B specimens are shown in Fig. 1 and also summarized in Table I. The remanent (σ_r) and saturation magnetization (σ_s) are almost equal in both specimens, 72 to 74 and 145 e.m.u. g^{-1}, respectively. The values of the ratio σ_r/σ_s are very close to 0.5 for both particles. The coercive force, however, principally yielded by external shape anisotropy, is higher in

* *Present address*: Department of Dental Materials, Tokyo Medical and Dental University, 1-5-45 Yushima, Bunkyo-ku, Tokyo 113, Japan.

0022–2461/88 $03.00 + .12

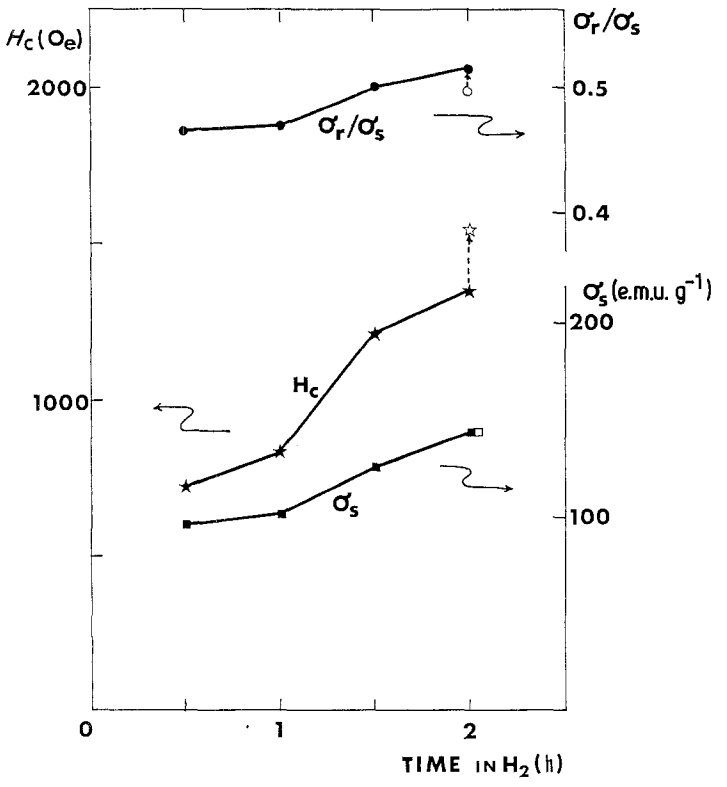

Figure 1 Change of coercive force (H_c), saturation magnetization (σ_s) and squareness ratio (σ_r/σ_s) with 400° C isothermal reduction time in a hydrogen atmosphere (series producing specimen A). For 2 h treatment, values of specimens A (●, ★, ■) and B (○, ☆, □) are compared.

the smaller particles (specimen B: 1540 Oe) than the larger particles (A: 1350 Oe).

Fig. 2 shows the bright-field image and selected-area diffraction patterns from the aggregates (left) and a single particle (right) for specimens A and B. The particle size on average expressed by a needle length is revealed to be 500 and 200 nm, respectively. Together with the heat treatment at 400° C the sharp needle shape of a starting material α-FeOOH becomes dulled besides the formation of pores inside a particle. The axial ratio of length to width of a particle is about 21 in larger particles (specimen A) and 10 in smaller ones (specimen B). For both sizes of particles the selected-area diffraction patterns from aggregates show the ring pattern of Fe with the broad ring of oxides [11] which infers the existence of oxides of the incomplete crystallization. The selected-area diffraction patterns from a single particle exhibits a definite difference. The pattern of specimen A is composed of the superposition of several single diffraction patterns indicating the existence of several grains inside, whilst that of specimen B shows a single crystal diffraction pattern. This was also confirmed by dark-field imaging technique, which verifies the area confined by diffraction contrast in a polycrystalline particle for specimen A and approximately uniformly bright area for a whole particle in specimen B.

TABLE I Comparison of the crystallographic and magnetic properties for the different size of single-domain iron particles

Properties	Specimen A	Specimen B
1. Crystallographic		
Particle size (nm^3)	24 × 24 × 500	20 × 20 × 200
Axial ratio b/a	21	10
Crystallinity	polycrystal	single crystal majority
Needle direction	random	[1 0 0] majority
Occupancy of [1 0 0] particles	1/9 (1 : single crystal)	20/29 (nearly 70%)
2. Magnetic		
Coercive force, H_c(Oe)	1350	1540
Saturation magnetization*, σ_s (e.m.u. g^{-1})	145	145
Remanent magnetization, σ_r (e.m.u. g^{-1})	74.7	72.2
Squareness ratio, σ_r/σ_s	0.515	0.498

*218 e.m.u. g^{-1} in bulk.

Typical examples of the electron micrograph and the corresponding diffraction pattern from a particle of specimen B are shown in Fig. 3. The diffraction pattern represents the [1 0 0] pattern of a body-centred-cubic iron in which the [2 0 0] direction is oriented parallel to a needle axis of a particle. The bright-field image shows the existence of pores inside a particle and variation of contrast, which shows the slight change of Bragg diffraction conditions [12]. These features indicate that crystallization is still incomplete. The ratio of [1 0 0] orientation of a needle axis is such that 20 out of 29 examples satisfy this relation, which corresponds to about 70%. In larger particles (specimen A), they are mostly polycrystals as shown above, and a rare example in which a single crystal is found to show a [1 0 0] needle axis. The data of crystallographic features for both specimens are summarized in Table I.

4. Discussion

On reduction of FeOOH to Fe, a decrease in volume of about 60% occurs. If the external shape of acicular particles is completely retained, the volume decrease would result in the formation of pores inside, which would cause harmful effects both in mechanical and magnetic properties. Using the heat treatment chosen

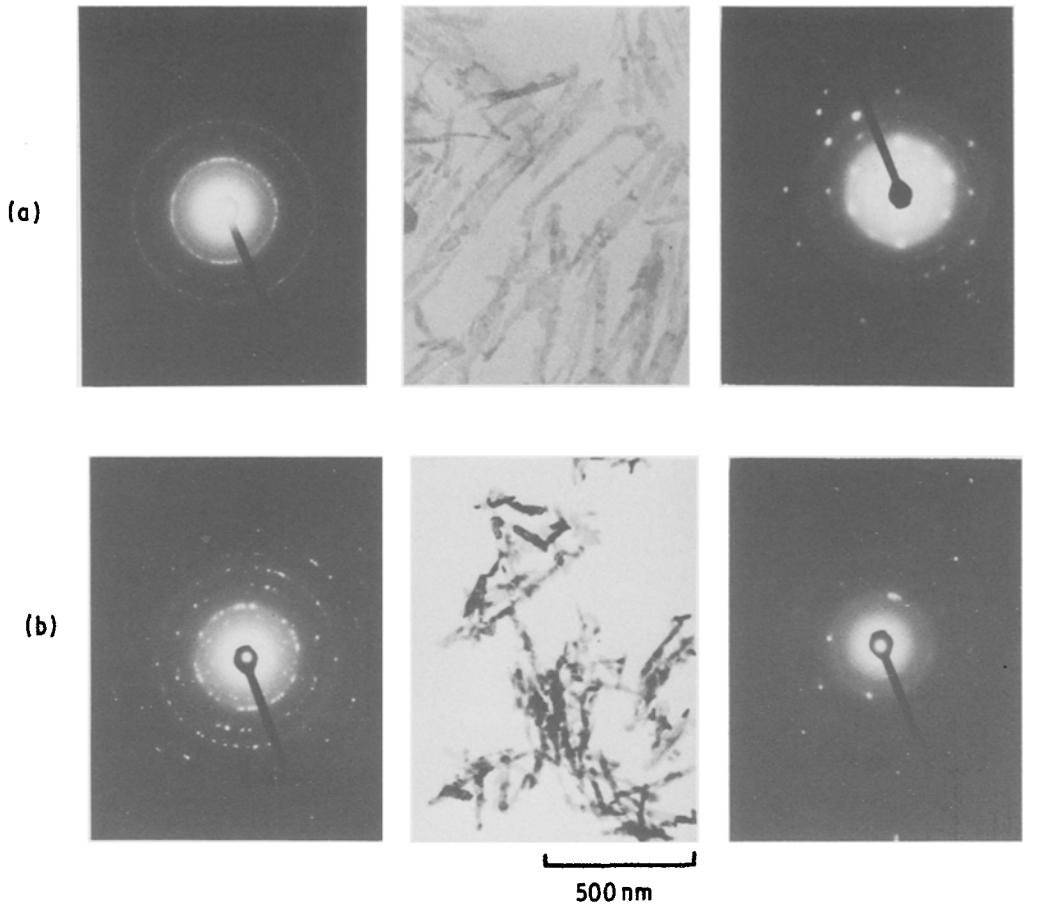

Figure 2 Effect of size on the crystalline properties in iron fine particles: (a) 0.5 μm, (b) 0.2 μm. Electron micrographs of fine particles (centre) and selected-area electron diffractions from aggregates (left) and a single particle (right).

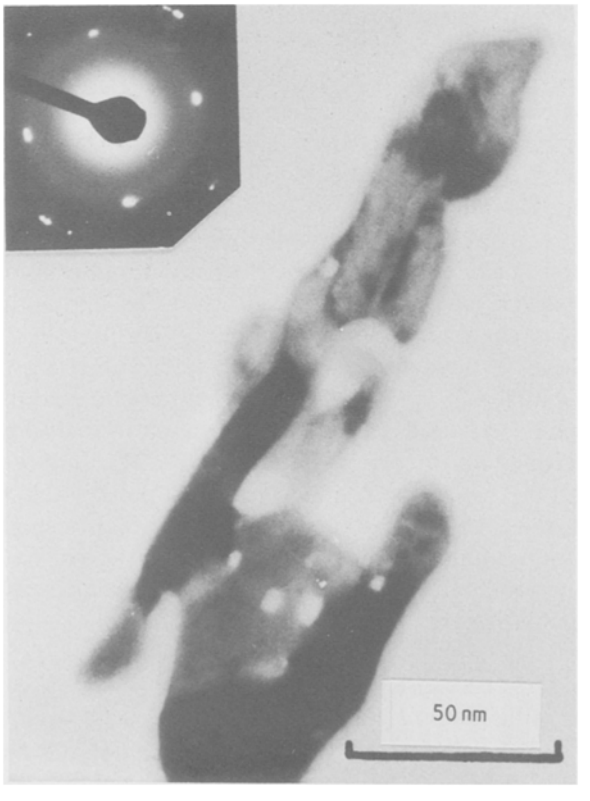

Figure 3 Typical electron micrograph of an iron fine particle (specimen B: average size 0.2 μm) showing single crystalline property and a [1 0 0] axial direction.

in the present experiment, the volume ratio of pores produced is much less than 60%, which ensures properties satisfactory for application. The reduction and the succeeding grain-growth process including surface diffusion re-forms acicular particles with a shape with less surface area, i.e. a shrinkage of the external shape with a progressively dulled needle shape resulting in a poorer axial ratio as well as a decrease in the volume ratio of the internal pores. The actual heat treatment condition is chosen by a compromise between the one to obtain better crystallization and that to conserve sufficiently good acicular shape.

The surface oxide layer of the present specimen has a thickness of ~ 3 nm from the estimation using Mossbauer measurements and X-ray diffraction [13]. Its crystal structure is very poorly crystallized or close to amorphous [11, 13].

The critical size for the single domain particle was calculated by Stoner and Wohlfarth [14], Kittel [15], Morrish and Yu [16], and others. According to Morrish [17], the critical size due to the shape anisotropy effect for the prolate spheroid with a radius in an equatorial axis a and a radius in a polar axis b is calculated by

$$a_c^2/[\ln (2a_c/u) - 1] = 6 J_e S^2/I_s^2 u N_a \qquad (1)$$

where the suffix c denotes the critical size, u is a cell

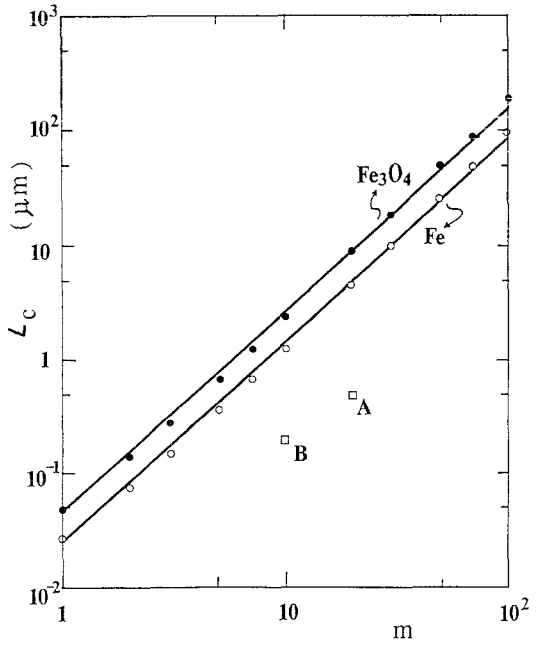

Figure 4 Critical particle size for single domain configuration (L_c) at an axial ratio (m) in iron and Fe_3O_4.

constant for the volume per atom or molecule, J_e is the exchange energy integral, S the spin quantum number, I_s the saturation magnetization in a unit volume, and N_a the demagnetization factor along the equatorial axis at an axial ratio m ($= b/a$). The results of calculation for iron, using the values $J_e = 156k$, $S = 1$ (k = Boltzmann's constant) after Kittel [15] and N_a calculated by Stoner [18], are shown in Fig. 4 together with those for Fe_3O_4. As is evident from the plot in a full logarithmic graph, the critical needle length, L_c ($= 2b_c$), is approximately proportional to the power of an axial ratio m

$$L_c = \alpha m^{\beta} \tag{2}$$

where α and β are material constants. This relation is expressed as $L_c = 2.3 \times 10^{-6} m^{1.8}$ for iron and $= 4.8 \times 10^{-6} m^{1.8}$ for Fe_3O_4. The situations for the present specimens are marked as A and B in the figure. The calculated critical domain sizes are approximately 5 and 1.5 μm for the axial ratio 21 (specimen A) and 10 (B). As easily recognized in Fig. 4, both specimens A and B sufficiently satisfy the conditions for a single domain configuration. The values of critical domain size are approximately ten times larger than the actual particle sizes 0.5 μm (A) and 0.2 μm (B).

According to Stoner and Wohlfarth [14], the random aggregates of single domain particles have a value of 0.5 for the squareness ratio σ_r/σ_s. The experimental values of squareness for iron fine particles are very close to 0.5 for both larger (A) and smaller (B) particles as shown in Fig. 1 and Table I. This is further support that the single domain configuration is realized for specimens treated in the present experiments. Thus although crystallographically there is a difference in that specimen A is a polycrystal and specimen B is a single crystal, both can be magnetically composed of single domain structure.

When the magnetic properties are examined for these two specimens in Fig. 1 and Table I, they are almost equivalent except for the coercive force. The origin of the difference in coercive force is considered below.

The coercive force, H_c, of a randomly oriented assembly of single domain particles with a cubic crystal structure and a prolate spheroid shape is represented as

$$H_c = 0.48(N_b - N_a)I_s + 0.64K/I_s + 0.48(3\lambda\sigma)/I_s - 1.7pI_s \tag{3}$$

where N_a and N_b are demagnetization coefficients along an equatorial and a polar axis, respectively, K is a magnetocrystalline anisotropic factor, λ is a magnetostriction constant, σ is the applied stress and p a packing factor. The first term represents the contribution of shape anisotropy [14], the second is that by magnetocrystalline anisotropy [19], the third is due to strain anisotropy [15], and the last is the interaction effect between packed particles [20].

Of the three possible causes of anisotropy, the effect of strain anisotropy would have little influence. Unlike the bulk specimen, the fine particles can easily cause strain relaxation because of their small size and large free surface. This is particularly true in the case of the present specimens which are undergoing shrinkage of their anisotropic external shape by recrystallization annealing. The contribution of strain anisotropy is estimated by Kittel [15] to be about 290 Oe for the applied stress 200 kg mm^{-2} but this is unlikely in the present case, as discussed above. We may omit the possibility for strain anisotropy in the following discussion.

The principal contribution to the realization of coercive force is given by shape anisotropy in the case of iron which has relatively small crystallographic anisotropy [15]. The strength of this coercive force depends on the axial ratio of the particles.

Calculation using Equation 3 gives rise to the values 5000 Oe at an axial ratio 21 (specimen A) and 4800 Oe at an axial ratio 10 (specimen B) for shape anisotropy. These theoretically estimated values are much higher than those experimentally obtained. This has been observed and discussed by several researchers [16]. The effect of packing causes the interaction among particles and works to lower the coercive force. This is particularly important when coercive force is mainly formed by shape anisotropy [15]. Further, iron fine particles used in the present study have the defects such as pores inside them and an oxide layer at the surface. Thus several factors exist to diminish the coercive force in the shape anisotropy effect. If the last term in Equation 3 (the packing effect) is taken into account, there is a decrease of coercive force of about 2000 Oe, which yields a value of approximately 2500 Oe. This is still twice as large as the experimentally obtained value of 1350 Oe. Although it is not possible at present to predict quantitatively the experimentally obtained value from theory, it clearly shows that the coercive force is mainly maintained by shape anisotropy. However, it does not explain the cause of the difference in the coercive force between specimens A (1350 Oe) and B (1540 Oe), especially the fact that

the higher value for coercive force is obtained for specimen B, in spite of its inferior axial ratio (10 to 21).

Therefore, it is necessary to consider effects other than strain anisotropy and shape anisotropy. Observation by electron microscopy revealed that larger particles (A) are polycrystalline and smaller ones (B) are mostly single crystals with the [1 0 0] needle orientation. In iron, [1 0 0] is an easy magnetization orientation [21]. It is then clear that there is a definite difference between A and B specimens in the intrinsic crystalline properties.

Kittel [15] estimated 160 Oe for the contribution by magnetocrystalline anisotropy, the second term of Equation 3. The experimentally observed difference in coercive force between smaller (B) and larger (A) particles is 190 Oe, which is in a good agreement with the theoretical estimation. Unlike shape anisotropy, the intrinsic magnetocrystalline anisotropy tends to be much less affected by packing effect. Thus it is suggested that the contribution of magnetocrystalline anisotropy might be one of the most important causes to produce a further increase in the coercive force in particles with a poorer axial ratio (specimen B).

5. Conclusion

Iron acicular fine particles of 0.2 and 0.5 μm needle length derived from α-FeOOH by reduction are both composed of single magnetic domain configuration. The coercive force is principally created by shape anisotropy. Unlike the 0.5 μm particles which are crystallographically polycrystalline, the 0.2 μm particles are single crystals whose major axis is oriented to the [1 0 0] direction, an easy magnetization direction of iron. This contributes to a further increase of the coercive force through magnetocrystalline anisotropy.

Acknowledgements

One of the authors (F.W.) thanks Professor S. Nomoto, Tokyo Medical and Dental University, for his generous encouragement to complete the research.

References

1. C. KITTEL, *Phys. Rev.* **70** (1946) 965.
2. G. W. VAN OOSTERHOUT, Proceedings International Conference on Magnetism, Nottingham, 1964 (Physical Society, London, 1965) pp. 529–32.
3. J. LIMA de FARIA, *Z. Kristallogr.* **119** (1963) 176.
4. FUMIO WATARI, J. VAN LANDUYT, P. DELAVIGNETTE and S. AMELINCKX, *J. Solid. State Chem.* **29** (1979) 137.
5. *Idem, ibid.* **48** (1983) 49.
6. FUMIO WATARI, P. DELAVIGNETTE and S. AMELINCKX, *ibid.* **29** (1979) 417.
7. FUMIO WATARI, J. VAN LANDUYT, P. DELAVIGNETTE, S. AMELINCKX and N. IGATA, *Phys. Status Solidi* **A73** (1982) 215.
8. G. W. VAN OOSTERHOUT, *Acta Crystallogr.* **13** (1960) 932.
9. P. BECKER, J. J. HEIZMANN and R. BARO, *J. Appl. Crystallogr.* **10** (1977) 77.
10. J. LIMA de FARIA, *Acta Crystallogr.* **23** (1967) 733 .
11. FUMIO WATARI, *Thin Solid Films* **97** (1982) 31.
12. P. B. HIRSCH, A. HOWIE, R. B. NICHOLSON, D. W. PASHLEY and M. O. WHELAN, "Electron Microscopy of Thin Crystals" (Krieger, New York, 1977).
13. K. HANEDA and A. H. MORRISH, *Surface Sci.* **77** (1978) 584.
14. E. C. STONER and E. P. WOHLFARTH, *Phil. Trans. R. Soc. (London)* **240A** (1948) 599.
15. C. KITTEL, *Rev. Mod. Phys.* **21** (1949) 541.
16. A. H. MORRISH and S. P. YU, *J. Appl. Phys.* **26** (1955) 1049.
17. A. H. MORRISH, "The Physical Principles of Magnetism" (Wiley, New York, 1965).
18. E. C. STONER, *Phil. Mag.* **36** (1945) 803.
19. L. NEEL, *Compt. Rend. Acad. Sci. (Paris)* **224** (1947) 1488.
20. D. F. ELDRIDGE, *J. Appl. Phys.* **32** (1961) 247S.
21. K. HONDA and S. KAYA, *Sci. Rep. Tohoku Univ.* **15** (1926) 721.

Received 20 March
and accepted 3 June 1987